Multiscale simulation of dynamic wetting

International Journal of Heat and Mass Transfer 115 (2017) 886–896

Contents lists available at ScienceDirect

International Journal of Heat and Mass Transfer

journal homepage: www.elsevier.com/locate/ijhmt

Multiscale simulation of dynamic wetting

Jun Zhang [a,*], Matthew K. Borg [b], Jason M. Reese [b]

[a] School of Aeronautic Science and Engineering, Beihang University, Beijing 100191, China
[b] School of Engineering, University of Edinburgh, Edinburgh EH9 3FB, United Kingdom

ARTICLE INFO

Article history:
Received 11 April 2017
Received in revised form 29 June 2017
Accepted 6 July 2017
Available online 1 August 2017

ABSTRACT

A sequential multiscale strategy that combines molecular dynamics (MD) with volume of fluid (VOF) simulations is proposed to study the spreading of droplets on surfaces. In this hybrid MD/VOF approach, VOF is applied everywhere in the domain with MD pre-simulations distributed along the wetted interface providing the crucial boundary information for the three-phase contact-line dynamics and the solid/liquid interfacial slip. For the latter, molecular shear flow simulations of the liquid in contact with the substrate are used to measure the local slip length to calibrate the Navier slip model. For the contact-line we use MD simulations of nanodroplets spreading on the substrate to calibrate the molecular kinetic theory (MKT) model for both the dynamic contact angle and the slip velocity. We validate this multiscale model for water nanodroplets spreading over a platinum surface by comparing our sequential hybrid simulations with the equivalent dynamics in a full MD treatment. We demonstrate that for nanodroplets spreading on surfaces, applying a dynamic contact angle model is not sufficient to pick up the molecular effects; we need to account for slip across the entire solid/liquid interface, in particular the large slip behaviour at the contact-line. We also demonstrate the application of this multiscale method to larger nanodroplets (up to ~100 nm diameters), where full MD simulation would be computationally intractable. We find that as the droplet size increases, the slip in the contact line region becomes less important. To simulate the full range of nano to macro droplets, an improved way of dealing with the VOF method is needed to reduce the overall number of grid points.

1. Introduction

Droplets spreading on a solid surface display fundamental dynamic wetting phenomena in which chemistry, physics, and mechanics intersect, and are also relevant for engineering applications such as coating, spray cooling, and inkjet printing [1]. Improvements in nanotechnology and nanofabrication over the past decade mean it is now possible to generate droplets down to nanoscales. In this research area, called "nanofluidics", an intriguing application is the direct printing of nanostructures on surfaces by electrostatic autofocusing of ink nanodroplets, as reported by Galliker et al. [2]. The spreading dynamics determines the evolution of the contact radius and hence the size of the nanostructure printed on a substrate.

While static wetting is well described by Young's contact angle equation, the dynamics of droplet wetting is more complicated as the physical processes in the local region near the moving contact line become important (for reviews, see Refs. [3,4]). It was first pointed out by Huh and Scriven [5] that the application to dynamic wetting of the Navier-Stokes equations with a no-slip boundary condition would lead to a stress singularity around the contact line. Different mechanisms have been proposed to address this problem, such as a slip boundary condition [5], a precursor film [6], an interface formation model [7], and molecular kinetic theory (MKT) [8,9].

Theoretically, a comprehensive understanding of the spreading process needs to consider surface tension, and viscous as well as inertial effects. In terms of numerical modelling, various methods have been used for dynamic wetting problems, such as volume of fluid (VOF) [10–13], level-set [14], and finite elements [15], to name just a few. In this paper, we choose the VOF method as the continuum-fluid simulation tool, since it has proven to be an efficient free-surface tracking technique and has been widely used in two-phase flows [16]. Key requirements in an accurate VOF simulation of a droplet spreading or impacting on a solid surface are the boundary conditions for the three-phase contact line as well as the solid/liquid interface. Slip boundary conditions and various dynamic contact angle models [11,13] have been implemented in VOF, and have been demonstrated to be important for the contact line dynamics. However, it is still not clear whether a slip boundary condition should be employed for the solid/liquid interface in the VOF method. More importantly, the slip behaviour around the three-phase contact line is still elusive. To the best of our

* Corresponding author.
E-mail address: jun.zhang@buaa.edu.cn (J. Zhang).

http://dx.doi.org/10.1016/j.ijheatmasstransfer.2017.07.034
0017-9310/

knowledge, there have so far been no VOF simulations incorporating models for the contact line slip. For macroscopic droplets, it seems that the various previous treatments of the boundary conditions can give acceptable results that compare well with experimental results. So it is difficult to evaluate which model is the most physically appropriate and well-founded.

The VOF method has been successfully applied to macroscopic droplet spreading and impact, however its applicability for nanodroplet spreading has not been investigated yet. At the nanoscale, molecular dynamics (MD) is the best computational tool to predict the dynamic wetting properties of nanodroplets. For example, Ritos et al. [17] investigated the dynamic wetting of water nanodroplets on moving silicon, graphite, and artificial superhydrophobic surfaces. Winkels et al. [18] performed two-dimensional MD simulations of the spreading of low-viscosity Lennard-Jones droplets on partially wetting surfaces with varying wettability, and compared the short time dynamics obtained by MD with high-speed empirical imaging of millimeter-sized water droplets. MD is a powerful tool for simulating nanodroplets, but using it to deal with macroscale droplets is impossible at present due to its computational intensity.

In this paper we apply a multiscale methodology to the spreading of droplets over a surface, as in the schematic in Fig. 1(a). To our knowledge, the only previous hybrid MD/continuum treatment of a water droplet on a surface has been reported by Wu et al. [19], who used the domain decomposition (DD) method [20] as shown in Fig. 1(b). In DD, the computational domain is divided into regions that need treatment using MD (e.g. near the triple-contact line point) and the remaining regions where a continuum treatment is accurate (e.g. in the bulk fluid). The MD and computational fluid dynamics (CFD) simulations then run concurrently in one simulation, exchanging flux and/or state properties regularly in time across an overlapping region. There are several discussions in the literature about why these concurrent hybrid simulations based on DD are not feasible for large-scale time-dependent problems [21,22], such as the case of a dynamically spreading droplet. As MD is computationally very expensive above length scales of a few nanometers and time scales of a few nanoseconds, a hybrid method using DD will still be intractable to evolve multiscale processes above these length and time scales — and long evolution timescales are required for larger drops. This is evident from the short time- and length-scales of nanodroplet spreading that were tackled by Wu et al. [19]. There are other issues that also arise in DD: the MD subdomains use unconventional and extremely challenging non-periodic boundary conditions; the problem of high statistical noise caused by low strain rates (affecting coupling, increasing algorithm instability, and restricting time-scale dependence); and the requirement to develop complex adaptive meshing procedures.

In this paper we instead propose a simpler and more effective multiscale method for dynamically spreading droplets, using a variant of the Heterogeneous Multiscale Method (HMM) [23] or, equivalently, the Equation-Free Multiscale Method [24]. In HMM, the computational flow domain is modelled by conventional CFD that is *concurrently* coupled with MD at every node of the domain to directly provide missing information either in the bulk (e.g. the stress field, if the fluid is an unknown non-Newtonian fluid) or at the boundary for nano/micro flow applications (e.g. to resolve the slip velocity). As such, there is then no need for closure equations for boundary slip or the stress variation with strain rate — hence the name 'equation-free'. In this paper we are dealing with water as the fluid, so there is only the need to resolve molecular effects near the wall, as shown in Fig. 1(c). Furthermore, the dynamics of water molecules is much faster than the transient dynamics of droplet spreading as a whole, so we can exploit this time-scale separation and use a cheaper and more convenient *sequential* approach. In a sequential approach [25], MD pre-simulations are first completed in order to gather variables over the parameter space of the particular problem. These are then implemented within the CFD solver through appropriate intermediate boundary or constitutive models, which means this approach is no longer 'equation-free'.

The remainder of this paper is structured as follows. The multiscale methodology is presented in Section 2, including the MD simulations, the standard VOF method and the coupling between MD and VOF through MKT and Navier slip boundary models. In Section 3, we first show calibration results for the MKT model using our MD simulations. We then compare the multiscale (i.e. our molecular-enhanced VOF) simulation results with the equivalent full-MD data of droplets spreading, and verify the most appropriate

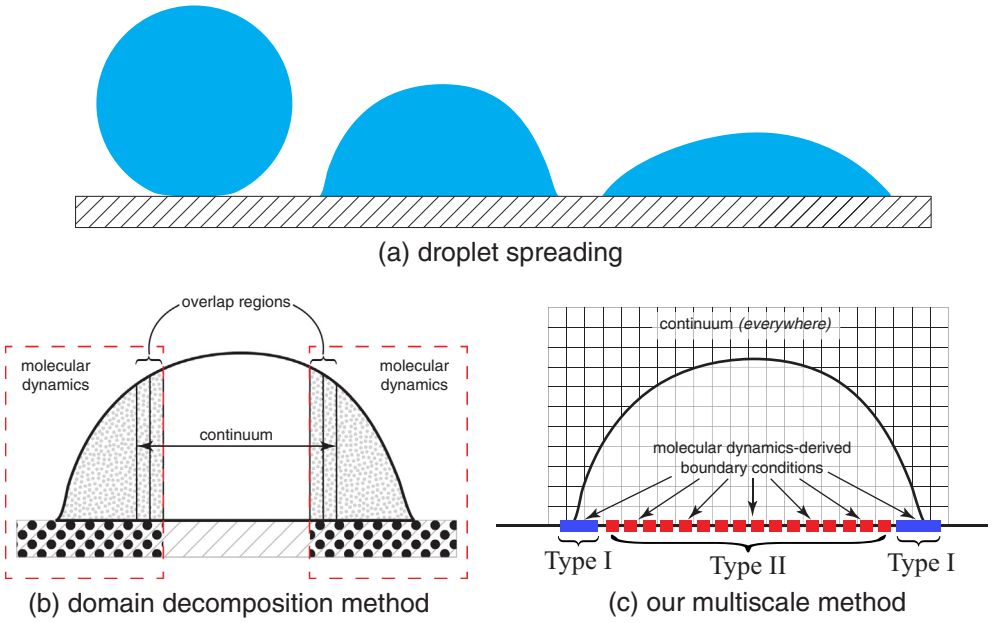

Fig. 1. Schematics of (a) a nanodroplet spreading on a surface, (b) treatment of this problem using domain decomposition [19], and (c) our multiscale approach.

boundary conditions for a corrected VOF simulation of spreading nanodroplets. Finally we demonstrate the full reach of these VOF simulations to larger nanodroplets that would not be accessible by MD, and study the effect of these boundary conditions on droplet size.

2. Multiscale methodology

In our multiscale method, the VOF method is applied over the entire macro flow region. The microscopic information at both the solid/liquid interface and the three-phase contact line region, which is required in order to capture the proper wetting behaviour of a spreading droplet on a substrate, is provided by MD subdomains distributed along the substrate interface, as depicted in Fig. 1(c). Each MD subdomain is coupled to a computational element (e.g. a face) on the macro grid boundary. As Fig. 1(c) indicates, there are two types of MD subdomains that are required to solve this coupled problem. We need one type of MD subdomain (which we will call Type I) to provide scaled-up information to the VOF solver about the dynamic contact angle and slip behaviour in the three-phase contact line region, and we need another type of MD subdomain (which we will call Type II) to provide information over the remainder of the solid/liquid interface.

This approach is an extension of the Heterogeneous Multiscale Method (HMM) [23] or equivalently, the Equation-Free Multiscale Method [24] to interfacial flows; originally the HMM was applied to single-fluid (i.e. argon) systems. In its present form, the standard HMM still presents unresolved challenges [26]. HMM typically applies MD subdomains at every computational node in the domain, and the CFD runs concurrently with MD; this means the VOF and MD solvers in this droplet case would need to exchange data dynamically to develop the overall macroscopic flow. This has three major limitations:

1. *Noisy data*: As the MD is run concurrently it provides statistically noisy information, such as pressure, stress or slip velocity, which may affect the overall algorithm stability, and require very lengthy averaging times.
2. *Unknown MD boundary conditions*: Resolving the moving interface in the Type I subdomain is extremely challenging (as indicated in the DD method of Wu et al. [19]), and the non-periodic MD boundary conditions for moving contact line problems are unresolved.
3. *Limitations on collocated nodes*: The MD subdomains need to be connected to all computational nodes (in this case along the surface of the substrate only), which presents a severe limitation on the grid size resolution, and hence the accuracy of the VOF. There is also the challenge of the varying number of MD subdomains as the droplet spreads and VOF adaptively refines the grid. This would create algorithmic demands for automated MD initialisation and processor load balancing.

While the fundamental HMM methodology is sound, the approach needs a better way to minimize the use of MD (the most expensive component of a hybrid simulation) for these interfacial problems. In this paper we propose a sequential approach (instead of a concurrent one) and use intermediate boundary models to link MD with VOF within the HMM framework. In many hybrid problems, the independent MD subdomain simulations are often very similar and repetitious, i.e., the molecular information that is collected is used once then wastefully discarded. This can be avoided in a sequential technique by simulating a series of different MD subdomains and building multidimensional libraries/interpolants to make meaningful predictions over expected parametric spaces, without the need for any further MD simulations.

We start by making the assumption that the slip behaviour at the solid/liquid interface (excluding the three-phase contact line region) can be obtained by MD simulations of shear flow, which will constitute our Type II subdomain. The Navier slip model, which relates slip velocity to the strain rate, can then be used as the intermediate model for VOF nodes. For an atomically smooth surface, the slip length is usually constant and so only one MD subdomain is required. For an inhomogeneous surface, multiple MD simulations would be needed to produce an interpolated field of the slip length.

For the three-phase contact line region, there are two issues related to the spreading dynamics; the first is the dynamic contact angle, which provides a geometric constraint for the spreading droplet, and the second is the slip, which might be much larger than that at the common solid/liquid interface, as demonstrated by Qian et al. [27] and Ren and E [28] theoretically and numerically, and by Qian et al. [29] experimentally. We assume that the MD simulations of nanodroplets spreading (our Type I subdomain) can provide enough information about the moving contact line. This data is used to determine the parameters in an intermediate model, such as the MKT model (as we explain below), which can then be employed to make predictions of larger droplets without the need for further MD simulations. For a droplet spreading uniformly over an atomically-smooth surface, the MD demand will therefore be just two types of simulations.

All our MD and VOF simulations are performed using the OpenFOAM software, which can be downloaded freely (www.github.com/micronanoflows). The mdFoam+ solver is a highly parallel MD code written by the authors, which has been validated across various micro/nano flow problems [17,30–33], including within our multiscale methods [22,26,34–36]. The interFoam solver is a VOF method that was first implemented in OpenFOAM by Ubbink [37]. Since its inception, it has undergone several modifications and has been widely applied to the simulation of multiphase flows [38,39]. Recently, the accuracy and efficiency of the interFoam solver have been evaluated approvingly by Deshpande et al. [40] using a variety of verification and validation test cases.

2.1. Molecular dynamics simulations

To determine the appropriate boundary conditions for the moving contact line, we perform MD simulations of water nanodroplets spreading on a platinum surface (which is our choice of substrate in this work) as shown in Fig. 2(a). This simulation setup is also used to validate our subsequent multiscale simulations of smaller droplets. The simulation domain is a cubic box of sides 25 nm, with periodic boundary conditions applied in all three directions. The platinum surface comprises 8 layers of atoms in an fcc structure (lattice constant 3.92 Å). The bottom four layers are fixed, while the atoms in the top four layers are coupled to a Berendsen thermostat to control the temperature at 300 K throughout the simulation. The initial condition consists of a pre-equilibrated spherical water droplet at 300 K placed just touching the platinum surface.

The MD simulation then proceeds until the droplet spreads over the surface and reaches a steady state. To obtain the temporal evolution of the contact radius and the contact angle during the spreading process, we first measure the two-dimensional density contours during the MD simulation. To do this, we use a cylindrical coordinate system (r, ϕ, y) that has the topmost solid surface layer as its zero reference level for the y direction and a normal line through the centre of mass of the droplet as its reference axis. Considering the axial symmetry of droplets, the three-dimensional density data are projected into two-dimensional bins (r, y) by averaging in concentric rings. The liquid/gas interface is defined by the points in the two-dimensional bins that have half the bulk density of the liquid phase. To extract the contact radius and contact angle

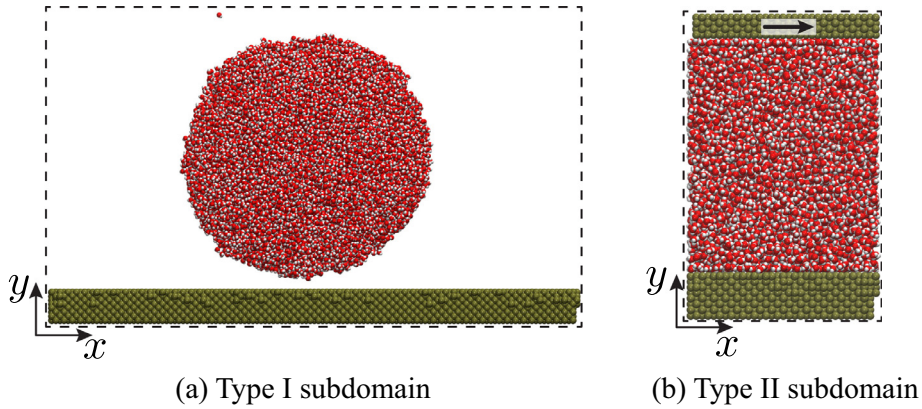

Fig. 2. Initial set-up of MD simulations for (a) nanodroplet spreading, and (b) Couette flow. The nanodroplet spreading model consists of a pre-equilibrated water droplet placed on a platinum surface. The distance between the top of the surface and the lowest part of the droplet is initially set at 0.4 nm. The Couette flow model consists of water molecules between two surfaces, with the top wall set to move at a constant velocity.

from the density contours, a popular method is to fit the liquid/gas interface to a circle [41]. However, the droplet shape is not always a spherical cap during the spreading process, especially at the initial stage, so we use a linear fit [42] instead. As shown in Fig. 3, a linear fit is made through the points of the liquid/gas interface in the range 6–12 Å above the solid surface. The contact angle is the angle formed between the linear fit line and the solid surface, and the contact radius is the distance from the centre of the droplet to the intersection of the linear fit line with the solid surface. For the cases we studied here, the equilibrium contact angle is around 40°.

To determine the slip behaviour at the common water/platinum interface, we perform MD simulations of a Couette flow, i.e. a water film 7.6 nm thick, confined between two parallel platinum walls, as shown in Fig. 2(b). The top wall moves with a fixed velocity of 100 m/s, and the bottom wall remains stationary. A Berendsen thermostat is applied to the velocity components normal to the flow direction, in order to maintain the system at 300 K. After the system reaches a steady state, the streamwise velocities are measured in bins distributed along the direction normal to the solid surface, and then the slip length can be determined straightforwardly according to the Navier slip model.

In all our MD simulations we use a velocity Verlet algorithm with an integration time step of 1.67 fs, and a cell-list algorithm for computing pair potentials. The rigid TIP4P/2005 model [43] is used to simulate the water molecules. It consists of one oxygen site O (no charge), two hydrogen sites H (0.5564 e), and one massless M site (−1.1128 e). The Lennard-Jones (LJ) pair potential is applied between oxygen sites with $\epsilon_{O-O} = 0.7749$ kJ mol^{-1} and $\sigma_{O-O} = 0.3159$ nm, while the Coulomb potential is applied between charge sites. Hamilton's quaternions are employed to keep the fixed geometry of the water molecules with an O-H distance of 0.09572 nm and an H-O-H angle of 104.52°. The LJ pair potential is also employed for the interactions between the non-fixed platinum atoms on the solid surface with the LJ parameters $\epsilon_{Pt-Pt} = 66.84$ kJ mol^{-1} and $\sigma_{Pt-Pt} = 0.2471$ nm [32]. The water/-platinum interactions are LJ pair potentials between the oxygen atoms and the platinum atoms with $\epsilon_{Pt-O} = 1.798$ kJ mol^{-1} and $\sigma_{Pt-O} = 0.2815$ nm [32]. Considering that the droplet is of finite size, and the semi-infinite solid surface carries no charge, the use of Ewald sums is not warranted [41]. Previous studies showed that a cutoff radius of 1.2 nm for both LJ and Coulombic forces can provide acceptable accuracy with computational efficiency [17,32,33], and so it is adopted here.

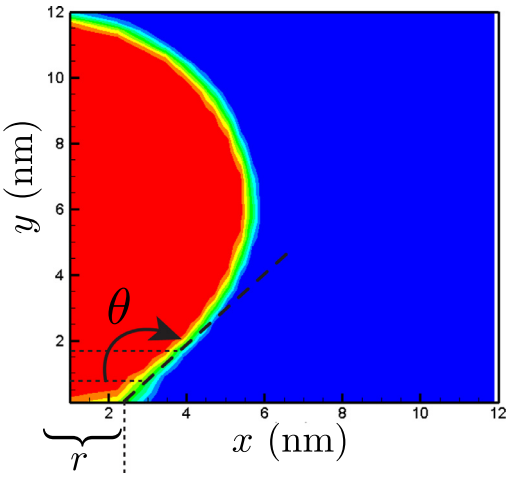

Fig. 3. Measurement of contact angle and contact radius. A linear fit is made through the points of the liquid/gas interface in the range 6–12 Å above the solid surface.

2.2. Volume of Fluid method

As a VOF solver, interFoam uses the volume fraction of the liquid phase (C) in each computational cell to track the interface. The volume fraction has a value of 1 or 0 when the cell is fully occupied by liquid or gas, respectively, and is in the range $0 < C < 1$ in the cells around the interface. The fluid properties, such as density ρ and viscosity μ, are weighted averages in each cell in terms of the volume fraction, viz.

$$\rho = \rho_l C + \rho_g (1 - C), \tag{1}$$

$$\mu = \mu_l C + \mu_g (1 - C), \tag{2}$$

where the subscripts l and g denote the liquid and the gas phases, respectively.

The governing equations within interFoam are for incompressible two-phase flows, and consist of the continuity equation, the advection equation of the volume fraction, and the momentum equation, as follows,

$$\nabla \cdot \boldsymbol{U} = 0, \tag{3}$$

$$\frac{\partial C}{\partial t} + \nabla \cdot (\boldsymbol{U} C) = 0, \tag{4}$$

$$\frac{\partial (\rho \boldsymbol{U})}{\partial t} + \nabla \cdot (\rho \boldsymbol{U}\boldsymbol{U}) = -\nabla p + \nabla \cdot \boldsymbol{\tau} + \boldsymbol{F}_\gamma, \tag{5}$$

where $\boldsymbol{U}$ is the velocity vector, p is pressure, $\boldsymbol{\tau}$ is the viscous stress tensor defined as $\boldsymbol{\tau} = \mu[(\nabla \boldsymbol{U}) + (\nabla \boldsymbol{U})^T]$, and $\boldsymbol{F}_\gamma$ is the surface tension force. In the VOF method, only a single momentum equation is solved, provided that in each cell the velocities for the two immiscible phases are the same.

The surface tension force $\boldsymbol{F}_\gamma$ is evaluated in terms of the gradient of the volume fraction, following the continuum surface force (CSF) model proposed by Brackbill et al. [44], i.e.

$$\boldsymbol{F}_\gamma = \gamma \kappa \nabla C, \tag{6}$$

where κ is the interface curvature, which is calculated based on the divergence of the unit interface normal $\boldsymbol{n}$, i.e. $\kappa = -\nabla \cdot \boldsymbol{n}$. The unit interface normal can be approximated as $\boldsymbol{n} = \nabla C/|\nabla C|$, except at the three-phase contact line where it is related to the contact angle via $\boldsymbol{n} = \boldsymbol{n}_w \cos\theta + \hat{\boldsymbol{t}}_w \sin\theta$, with $\boldsymbol{n}_w$ the unit normal to the wall, $\hat{\boldsymbol{t}}_w$ the unit normal to the contact line formed between the liquid/gas interface and the wall, and θ is either the static or dynamic contact angle, which is specified as a boundary condition.

2.3. Coupling through molecular kinetic theory

We choose molecular kinetic theory (MKT) as the intermediate boundary model to correct the VOF model for contact angle and slip velocity in the contact line region. MKT has been applied to a variety of dynamic wetting problems and has been validated by comparing with experimental data [9,45]. The principal hypothesis of MKT is that the dynamics of the contact line is determined by the statistical kinetics of molecular events occurring within the three-phase zone, where the solid, liquid, and gas phases meet. When fluid advances on a solid surface, the molecules previously adsorbed at localized sites on the initial solid/liquid interface are displaced by the molecules from the advancing fluid. So MKT can be considered as an adsorption/desorption model. The key parameters are κ_w^o, the equilibrium frequency of the molecular displacements, and λ, the average distance of each displacement.

According to Eyrings theory of absolute reaction rates, κ_w^o is related to the specific activation free energy of wetting Δg_w^* [8], i.e.

$$\kappa_w^o = \frac{k_B T}{h} \exp\left(\frac{-\Delta g_w^*}{n k_B T}\right), \tag{7}$$

where k_B, h, and T are the Boltzmann constant, Planck constant, and absolute temperature, respectively, and n is the number of adsorption sites per unit area on the solid surface. When the system is at equilibrium, although the thermal motion of molecules always exists, the net rate of displacement is zero because the frequency of molecular displacements in the forward direction κ_w^+ is equal to that in the backward direction κ_w^-, i.e. $\kappa_w^+ = \kappa_w^- = \kappa_w^o$.

However, when the wetting contact line advances along the solid surface, the adsorption/desorption equilibrium is broken. As a result, a driving force around the three-phase zone for the contact line to move is generated. The force modifies the frequency of the molecular displacements, increasing κ_w^o to κ_w^+ in the forward direction and reducing it to κ_w^- in the backward direction. The contact line therefore moves to relieve the force at an average velocity $V = \lambda(\kappa_w^+ - \kappa_w^-)$.

MKT assumes that the driving force F_w for the contact line to move can be estimated from the out-of-balance surface tension force, i.e. $F_w = \gamma(\cos\theta_s - \cos\theta_d)$. Here, γ is the surface tension of the liquid, and θ_s and θ_d are the static and dynamic contact angles, respectively. On this assumption, the contact line velocity is [8]

$$V = 2\kappa_w^o \lambda \sinh\left(\frac{\gamma(\cos\theta_s - \cos\theta_d)}{2 n k_B T}\right). \tag{8}$$

It can be seen from this equation that the magnitude of the contact line wetting velocity increases with the deviation between the dynamic and static contact angles. For the case of a droplet spontaneously spreading, the dynamic contact angle changes from 180° when the droplet just touches the solid surface, to the static value at equilibrium; so the contact line velocity is maximum at the initial time and tends to zero as the droplet approaches its equilibrium shape.

Alternatively, Eq. (8) can be written in terms of the dependence of dynamic contact angle on the contact line velocity, i.e.

$$\cos\theta_d = \cos\theta_s - \frac{2 n k_B T}{\gamma} \sinh^{-1}\left(\frac{V}{2\kappa_w^o \lambda}\right). \tag{9}$$

Using the dimensionless capillary number $Ca = \mu V/\gamma$ (where μ is the liquid viscosity) to replace the velocity V, this equation becomes

$$\cos\theta_d = \cos\theta_s - \frac{2 n k_B T}{\gamma} \sinh^{-1}\left(\frac{Ca}{2\kappa_w^o \lambda \mu/\gamma}\right). \tag{10}$$

Note that Eqs. (8) and (10) are two ways of describing the MKT model. Eq. (10) is a dynamic contact angle model, which has been widely used in continuum simulations as a geometrical boundary condition to provide time-dependent contact angles. Eq. (8) provides a mechanism to generate slip velocity at the three-phase contact line. The latter has been overlooked previously because slip is normally negligible for macro droplets. In nanodroplets this slip mechanism can, however, dominate the spreading dynamics. Therefore, we exploit both these equations in our numerical implementation. As Eqs. (8) and (10) are actually the same MKT model written either in terms of V or θ_d, we need a way of decoupling each equation using independent information already determined by the VOF simulation.

Specifically, at every time step of the VOF simulation, the dynamic contact angle $\theta_d(t)$ as a geometrical boundary condition is calculated using Eq. (10), where the velocity V is assumed as the velocity $u_c(t)$ in the cell-centre close to the contact line, as shown in Fig. 4(a). The slip velocity at the boundary face is then calculated using Eq. (8), but rather than using the value of the contact angle $\theta_d(t)$ calculated from Eq. (10) as an input, we measure the instantaneous contact angle using the same technique as in the MD simulation, i.e. producing a contour plot of density (as computed by the VOF solver), then fitting a line through the liquid/gas interface and measuring θ in the region 6–12 Å above the solid surface. Inputting the instantaneous dynamic contact angle θ into Eq. (8), we can determine the slip velocity $V = u_s^{\mathrm{MKT}}$, as shown in Fig. 4(b).

Note that these MKT equations contain constants that are dependent on the chemistry and structure of the substrate, and so are obtained from our Type I MD pre-simulations, as we describe in more detail below.

2.4. Coupling through Navier slip

We choose the Navier slip model [46] as the intermediate boundary model that corrects the VOF for the solid/liquid slip, which is given by:

$$u_s^{\mathrm{N}} = l_s \frac{\partial u}{\partial y}, \quad \text{at} \quad y = 0, \tag{11}$$

where u_s^{N} is the Navier slip velocity parallel to the solid surface, and l_s is the slip length. In a pure shear flow, l_s can be interpreted as the fictitious distance into the surface where the no-slip boundary condition would be satisfied. The value of the slip length for a solid/liquid interface can be determined by experiment [46] or MD simulations [47]. In our multiscale approach, the value for l_s is

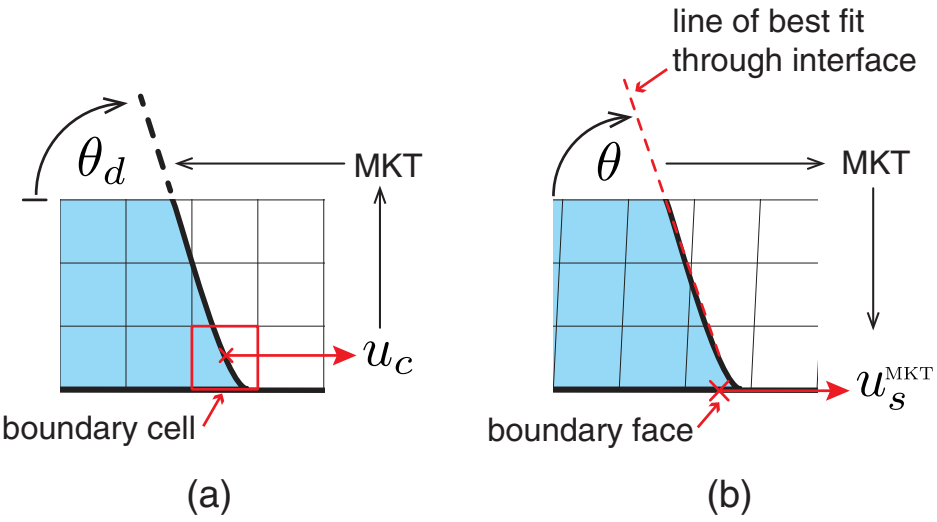

Fig. 4. Schematic of our numerical implementation imposing both the dynamic contact angle and the slip velocity at the triple-contact-line region in a VOF simulation. (a) The dynamic contact angle as a boundary condition is determined from the cell-centre velocity closest to the contact line, $V = u_c$ in Eq. (10). (b) The slip velocity as a boundary condition is determined from the direct measurement of the instantaneous dynamic contact angle θ, which is obtained from a linear fit to the liquid/gas interface and then used with Eq. (8) to determine $V = u_s^{\mathrm{MKT}}$.

determined from our Type II MD simulations of Couette flow using Eq. (11) in conjunction with our measured strain rate. For water over platinum, our MD pre-simulations produce l_s = 0.28 nm (which is measured from the first layer of water molecules so as to be consistent with the VOF method). Note, generally l_s is constant for a given substrate and is independent of strain rate; it only diverges beyond a critical strain rate, but this is much larger than what these droplets experience.

3. Results

3.1. Full MD simulations and MKT calibration

In this section we employ full MD simulations as benchmark cases for comparison with our multiscale simulations. Three different sizes of water nanodroplets containing 8000, 15,625, and 27,000 water molecules, respectively, are simulated. The initial droplet radii R_0 are 3.8 nm, 4.7 nm, and 5.6 nm, respectively, and Fig. 5 shows snapshots from the full MD simulations of their spreading on the platinum surface. The initial contact angle ($\theta = 180^\circ$) gradually changes to the static contact angle ($\theta_s = 40^\circ$), which is determined by the interaction strength between the platinum atoms and the water molecules.

During the simulation, temporal evolutions of the density distributions are obtained in two-dimensional bins every 10,000 MD time steps. The contact angle and contact radius are then determined from the density distributions according to the method presented in Section 2.1. Fig. 6 shows the temporal evolution of the contact radius and contact angle, where the time is normalised by the characteristic inertial time $(\rho R_0^3/\gamma)^{1/2}$, and the contact radius is normalised by the initial droplet radius R_0. It can be seen that all these three sets of data collapse onto one curve for both contact radius and contact angle, which indicates that for nano-sized droplets the spreading dynamics is similar.

With this data we follow the standard method of Bertrand et al. [48] to calibrate the dynamic contact angle model for the water/-platinum system. First the temporal evolution of the contact radius $r(t)$ shown in Fig. 6(a) is fitted by a ratio of polynomials:

$$r_{\mathrm{fit}}(t) = \frac{\sum_{k=0}^{k_{\max}} a_k t^k}{1 + \sum_{k=1}^{k_{\max}} b_k t^k}. \tag{12}$$

Here, a_k and b_k are the free parameters to be adjusted, and $k_{\max}$ is set as 10 [48]. From this analytical expression, the contact line velocity $V(t)$ can be obtained by simple differentiation $V(t) = dr_{\mathrm{fit}}(t)/dt$, and hence the capillary number is determined. For time t, we now have the measured dynamic contact angle $\theta_d(t)$ and the calculated capillary number $Ca(t)$. The complete set of $\theta_d(t)$ and $Ca(t)$ data are then fitted to the MKT model:

$$\cos\theta_d = \cos\theta_s - A\sinh^{-1}\left(\frac{Ca}{B}\right), \tag{13}$$

where A and B are the parameters to be determined by the fitting. Fig. 7 shows that the curve of Eq. (13) with $A = 0.94$ and $B = 0.17$ fits our MD data very well. So this dynamic contact angle model is used as a boundary condition in our subsequent VOF simulations.

3.2. Multiscale simulations of nanodroplets spreading

The accuracy of the hybrid MD/VOF solver in simulating water nanodroplets spreading is now considered by comparison with the full MD simulations. As the results for the three nanoscale droplets are very similar, all results that follow in this section are for the 5.6 nm radius droplet.

To save computational time, the VOF simulation is set up as a two-dimensional axisymmetric system. The computational domain is square with side length 33.6 nm. The size of the droplet is chosen to be the same as in the full MD benchmark case (i.e. 5.6 nm). Initially the droplet is set just touching the solid surface, with its centroid on the axis of symmetry. The remainder of the simulation box is full of air. For a fair comparison between the VOF and MD results, the physical properties of water in the VOF solver are chosen to be consistent with those in the MD simulations. Previous MD studies have demonstrated that the density, viscosity, and surface tension of water using the TIP4P/2005 model at 300 K are 996.5 kg/m^3 [43], 0.84 mPa s [49], and 63.9 mN m^{-1} [32], respectively. These values are used in our VOF simulations. Considering the size of the droplet, the effect of gravity is negligible.

The whole computational domain is divided into a uniform grid of 256 × 256 cells. The time step is controlled by setting the maximum Courant number to be 0.1. During the spreading process, the water/air interface is determined on-the-fly by the isosurface of

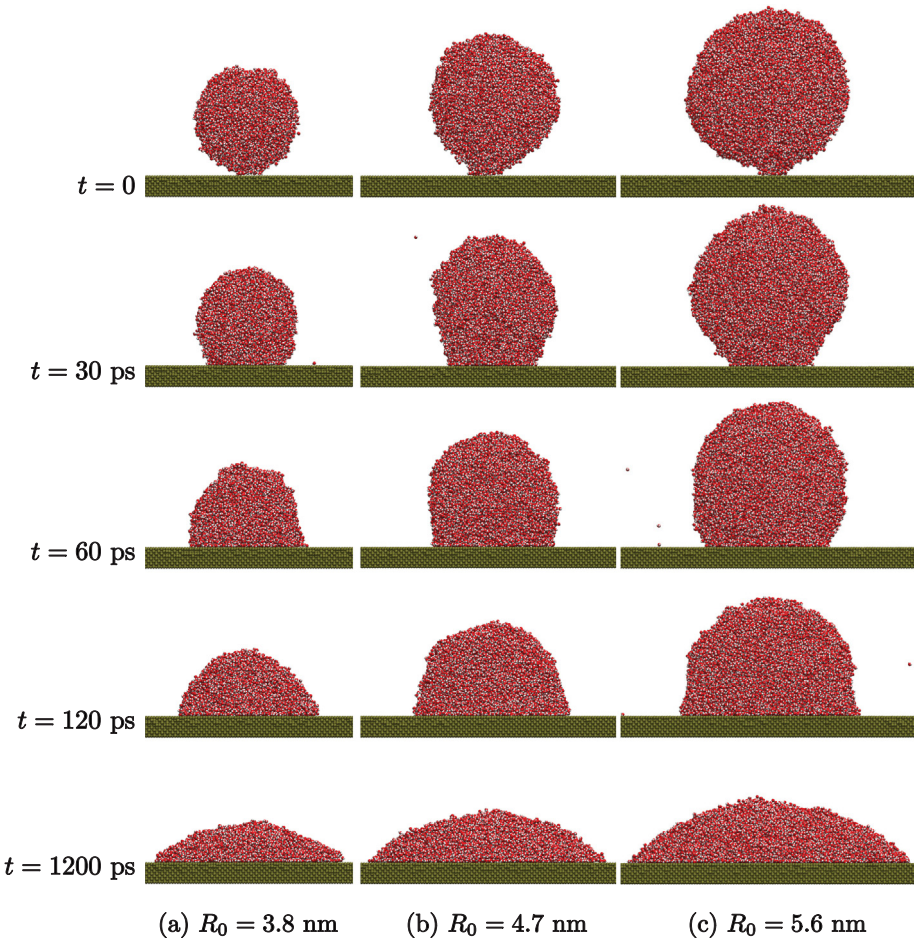

Fig. 5. Snapshots of cross-sections of full MD simulations of droplets spreading on a platinum surface.

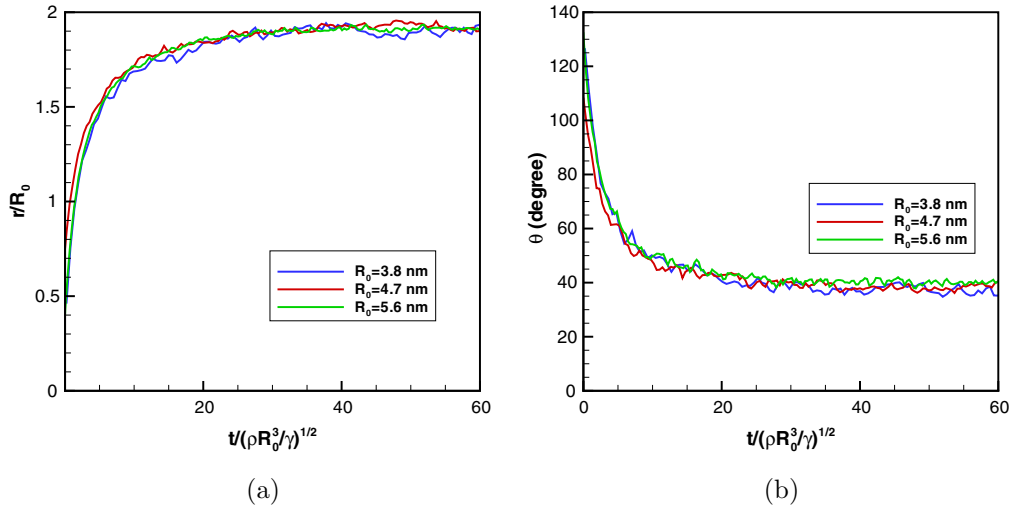

Fig. 6. Normalised temporal evolutions of (a) contact radius and (b) contact angle.

the volume of fraction with $C = 0.5$. The interface data are output every 20 ps. The temporal evolutions of the contact radius and the contact angle are then obtained from the measured interface using the same method as that used in the previous MD simulations.

To assess the three boundary conditions in our multiscale simulation — i.e. VOF with Navier slip, MKT slip and dynamic contact angle – as compared to the benchmark MD simulation, we carried out the following sensitivity studies:

(A) Apply the VOF solver with a dynamic contact angle and the entire solid/liquid surface assumed as no-slip;

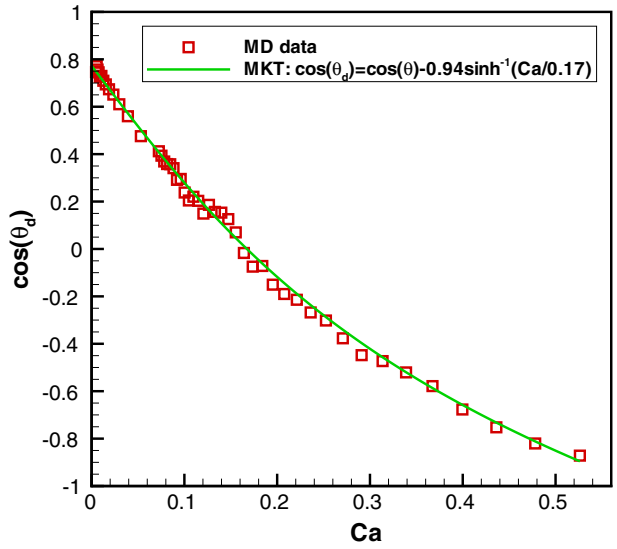

Fig. 7. MKT dynamic contact angle model fitted to MD data of nanodroplets spreading with initial radii 3.8 nm, 4.7 nm, and 5.6 nm.

(B) Apply the VOF solver with a dynamic contact angle and the entire solid/liquid surface given a Navier slip;
(C) Our multiscale method: apply the VOF solver with a dynamic contact angle, the MKT slip at the three-phase contact line region obtained from our Type I MD subdomain, and a Navier slip obtained from our Type II MD subdomain applied in the remaining solid/liquid region.

For study (A), Fig. 8 compares the VOF results with MD data for the spreading dynamics. The black solid line is the MD data, and the green square symbols are the VOF result with the no-slip boundary condition and a dynamic contact angle model. It is clear that the VOF solver predicts much slower spreading than the MD result. For study (B), we tested the influence of slippage at the surface by including a Navier slip model with varying slip lengths at the entire solid/liquid interface, starting with the reference slip length l_s = 0.28 nm which we found from our MD pre-simulation,

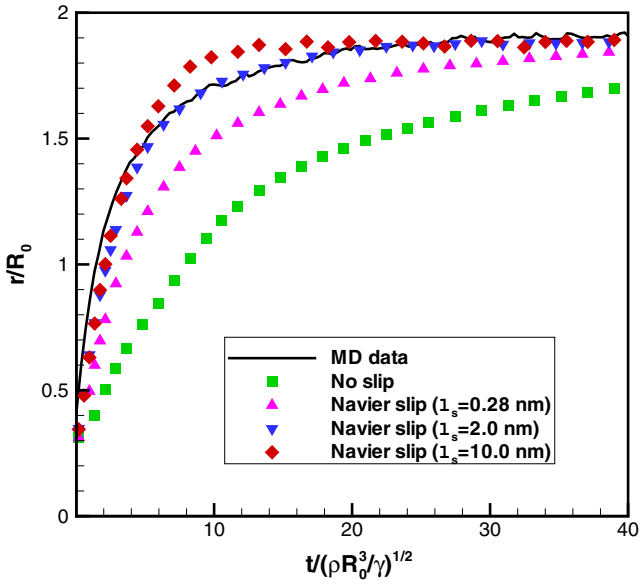

Fig. 8. Comparison of VOF and MD results of normalised temporal evolutions of the contact radius. In the VOF simulations, the Navier slip model is used as a boundary condition over the entire solid/liquid interface.

and then increasing this up to 10 nm. These results are also shown in Fig. 8. We find that the droplet spreading rate increases with the slip length. For example, when the slip length is set to 2 nm, the VOF result seems to match the MD data, except in the initial stages of spreading. Larger slip lengths (e.g. l_s = 10 nm) give faster spreading than MD after a short time period.

Similar matching studies between MD and continuum phase field methods for nanodroplets have also been done by Nakamura et al. [50] and Johansson et al. [51], and they claimed that the continuum phase-field result can match MD results very well if the slip length in the Navier slip boundary condition or the contact line friction parameter is adjusted. However, the slip length is not an arbitrary numerical parameter but has a physical value for a specific solid/liquid interface configuration. As we found using Couette flow simulations, the slip length for this water/platinum interface is 0.28 nm, so there is some missing physical understanding between this slip length and the value of 2.0 nm which is required to make the VOF result match better with MD. The reason for this inconsistency is that the apparent slip length at the contact line is much larger than the intrinsic slip length. This behaviour has been recently demonstrated experimentally [29]. A possible but unsatisfactory solution is to employ the Navier slip model with a varying slip length along the solid/liquid interface. However, it is difficult to know what the slip length at the contact line is *a priori*.

In study (C) we use our multiscale approach. This applies VOF with the MKT slip model in the three-phase contact line region (i.e. we do not apply Navier slip in this region), but the Navier slip model with l_s = 0.28 nm for the rest of the solid/liquid interface. The interpretation of the MKT slip model is that if the dynamic contact angle deviates from the static value, there is an unbalanced Young's force around the contact line, and this generates a slip velocity. To apply this interfacial slip, we use the calibrated slip equation (as described above):

$$u_s^{\mathrm{MKT}} = \frac{B\gamma}{\mu}\sinh\left(\frac{\cos\theta_s - \cos\theta_d}{A}\right), \tag{14}$$

where the values of A and B are the same as those determined for Eq. (13), and γ and μ are the surface tension and viscosity of water, respectively.

In the VOF method, the interface is sharp and defined numerically across three computational cells, with the volume fraction (C) changing from 0 to 1 within this region. On the other hand, in MD simulations, the contact line region has a physical width w, in which the density changes from vapour to bulk liquid. To match the VOF simulations to the full MD, the MKT slip velocity u_s^{MKT} is applied only to those boundary faces located within the contact line region, i.e. within $w/2$ in the direction parallel to the surface from the contact line. The width of the contact line region measured from our MD simulations is about 1.7 nm.

Fig. 9 shows our multiscale results (red squares), i.e. a VOF simulation with MKT slip in the contact line region (w = 1.7 nm) and Navier slip (l_s = 0.28 nm) on the remainder of the solid/liquid interface. Our multiscale results agree very well with the MD spreading results over the whole time-scale, including the initial spreading response. In order to check the sensitivity to w in our model, we have run simulations using the same model but with w = 0.4 nm and w = 1.0 nm. The results are also plotted in Fig. 9; it can be seen that the results obtained using these two artificial values of the parameter slightly underestimate the spreading rate, although they still produce much better results than any of the other approaches we have tried.

As a further demonstration, in Fig. 10 we compare cross-sectional snapshots of nanodroplet spreading obtained by our multiscale method with those from MD. The left hand sides of the images are the snapshots at different times in the full MD, while

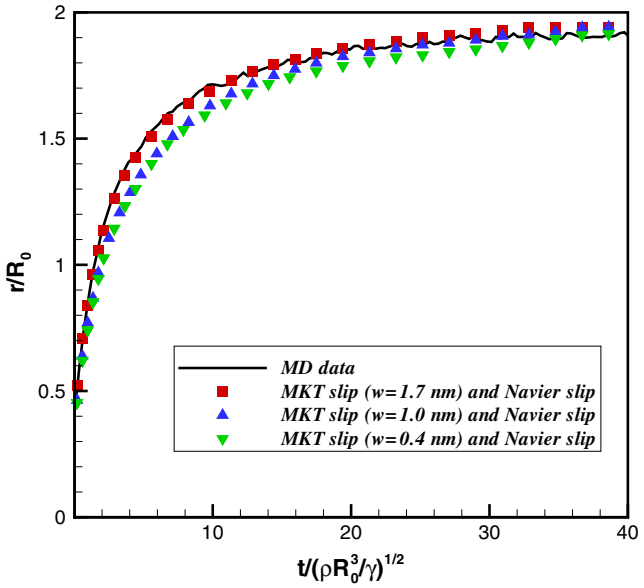

Fig. 9. Comparison of multiscale and MD results of normalised temporal evolutions of the contact radius. In the multiscale VOF simulations, the MKT slip model is used for the contact line region, while the Navier slip model (l_s = 0.28 nm) is used for the remainder of the solid/liquid interface. Three multiscale results obtained using different widths w of the contact line region are shown for comparison.

the right hand sides are the corresponding snapshots from the VOF solver (i.e. the volume fraction of water). The red region is the liquid bulk phase, while the blue region is the gas bulk phase. It can be seen that the overall droplet properties (e.g. radius, height, curvature) obtained by these two different simulation methods are quite similar. For this case, the computational cost for the VOF multiscale simulation is around 13 times less than for the MD simulation.

3.3. Multiscale simulations of the spreading of larger nanodroplets

For a specified solid/liquid interface, the interatomic potential and interaction strength in MD simulations remain constant, no matter how large the droplet is. However, using MD to simulate macroscopic droplets is unrealistic at present due to the massive computational resource requirements. On the other hand, there is no such limitation on VOF simulations, as the need for computational memory is dependent on the number of computational grid cells but not the number of molecules. Since the multiscale VOF method has been validated for nanodroplets in the previous section, it is natural to extend the VOF simulations to assess their value in predicting larger nanodroplets.

As the size of the droplet increases, the area where the MKT slip is applied becomes smaller relative to the area where the Navier slip is applied, so the effect of MKT slip on the spreading dynamics becomes less important. To identify the droplet size dependence of the effect of MKT slip, we compare the results for R_0 = 10 nm,

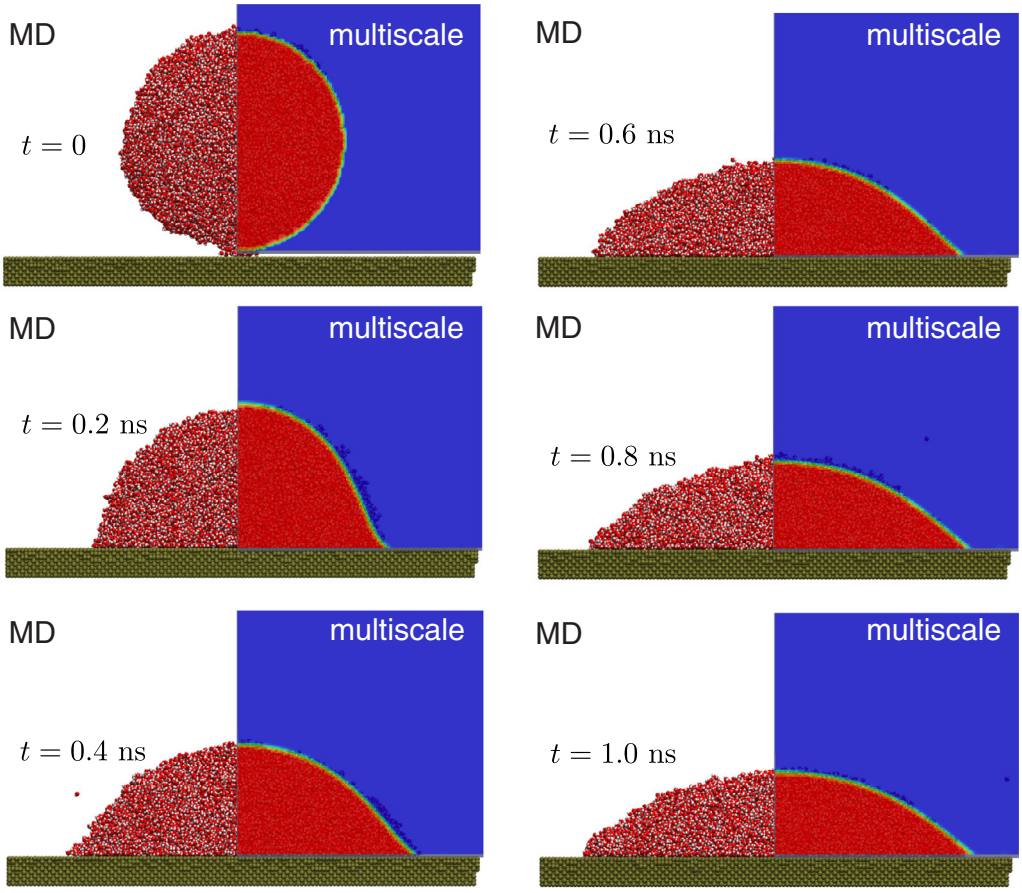

Fig. 10. Comparisons of cross-sectional snapshots in the spreading of a nanodroplet of radius 5.6 nm obtained by full MD simulations (left hand side in each column) and our multiscale VOF/MD method (right hand side in each column). In our multiscale simulation, we use the MKT slip model for the contact line region (w = 1.7 nm) and the Navier slip model (l_s = 0.28 nm) for the remainder of the solid/liquid interface.

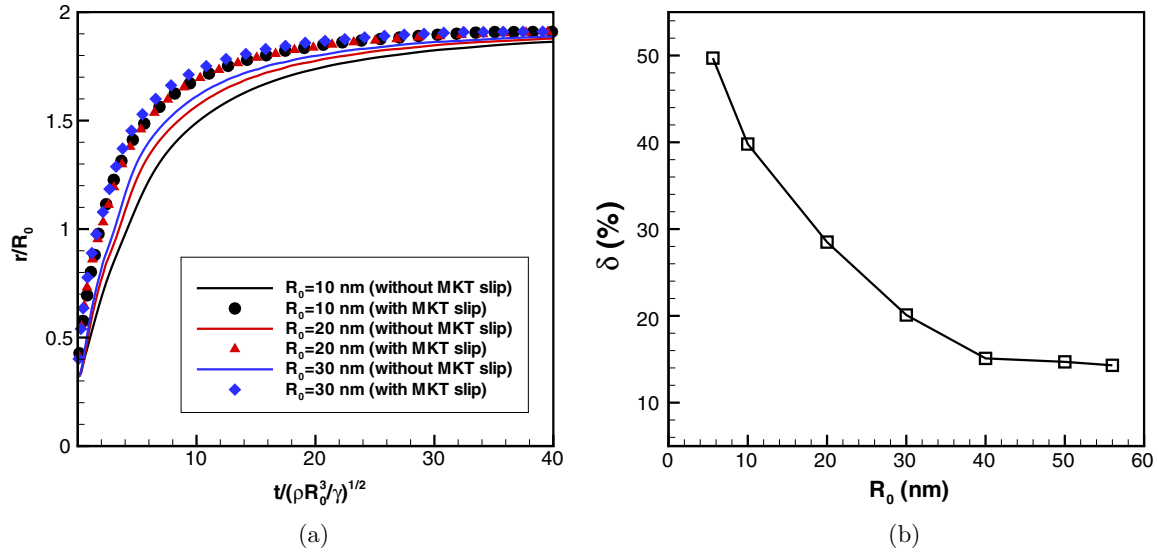

Fig. 11. Effect of MKT slip on the droplet spreading. (a) Comparison of the temporal evolution of the contact radius both with and without the MKT slip boundary condition, for different sized droplets. (b) The relative error δ versus droplet radius.

20 nm, and 30 nm obtained using two different sets of slip boundary conditions. The first one has MKT slip in the contact line region (w = 1.7 nm) and Navier slip (l_s = 0.28 nm) in the remainder of the solid/liquid interface. The second set applies only Navier slip (l_s = 0.28 nm) over the entire solid/liquid interface. Fig. 11(a) compares the normalised contact radius as a function of the normalised time obtained by the multiscale simulations. Without MKT slip, the spreading rate increases with the droplet size. However, if MKT slip is used in the contact line region instead of the Navier slip model, the spreading rates are almost the same for these three different sizes of droplets: the spreading dynamics for all nanoscale droplets is similar.

To quantify the size dependence of the effect of the MKT slip, we define a characteristic time scale t_e at which the contact radius reaches 95% of its maximum value. Correspondingly, t_e^N is the t_e obtained only using the Navier slip boundary condition, while t_e^M is the t_e obtained using both Navier and MKT slip boundary conditions. The relative error between these is:

$$\delta = \frac{t_e^N - t_e^M}{t_e^N} \times 100\%. \tag{15}$$

As shown in Fig. 11(b), the relative error δ decreases with initial droplet size. For the case of a droplet of radius 10 nm, the effects of the MKT and Navier slip models are of the same magnitude (evident from the 50% influence of MKT on the results). However, when the initial droplet radius is 40 nm, the relative error is reduced to 15%.

In principle, we can apply our multiscale approach to even larger droplets, but the VOF solver needs many more grid points to do so. Previous VOF studies [12] have demonstrated that there is an implicit (or numerical) slip length proportional to the size of the grid cell closest to the solid surface. Therefore, an accurate VOF simulation needs a mesh size smaller than the intrinsic slip length, otherwise the implicit slip length dominates. Considering that the intrinsic slip length in our simulation cases is only 0.28 nm, if we simulate a droplet with a radius of 1 mm, the required grid points in one direction are as large as 3,600,000; this is intractable, even for current supercomputing resources. A possible solution to reducing this computational cost is to apply adaptive and local mesh refinement, and this will be the subject of future work.

4. Conclusions

We have proposed a new multiscale method that combines both MD and VOF methods sequentially to study water droplets spreading on a platinum surface. We demonstrated that, besides a dynamic contact angle model, an MKT slip model for the contact line region and a Navier slip model on the remainder of the solid/liquid interface are needed if VOF simulation results are to be consistent with MD data for the spreading of nanodroplets.

We then extended the VOF simulations to the spreading of larger nanodroplets. The effect of the MKT slip model becomes less important as the droplet size increases. When the initial droplet radius is above 40 nm, the difference between results obtained with and without the MKT slip model is less than 15%.

The sequential hybrid MD/VOF method described in this paper provides a general way to study the multiscale dynamics of wetting. Other applications of liquid droplets spreading or impacting on any solid surfaces, ranging from hydrophilic to hydrophobic, can be studied using the method we have presented here.

Conflict of interest

Authors declare that there is no conflict of interest.

Acknowledgements

We thank James Sprittles and Terence Blake for stimulating discussions. This work is financially supported by the UK's Engineering and Physical Sciences Research Council (EPSRC) under Grant Nos. EP/K038621/1 and EP/N016602/1. MKB and JMR also acknowledge the ARCHER Leadership grant that enabled the molecular dynamics simulations to be run on ARCHER, the UK's national supercomputing service. All data within this publication can be freely accessed at: (http://dx.doi.org/10.7488/ds/2077).

References

[1] D. Bonn, J. Eggers, J. Indekeu, J. Meunier, E. Rolley, Wetting and spreading, Rev. Mod. Phys. 81 (2) (2009) 739.
[2] P. Galliker, J. Schneider, H. Eghlidi, S. Kress, V. Sandoghdar, D. Poulikakos, Direct printing of nanostructures by electrostatic autofocussing of ink nanodroplets, Nat. Commun. 3 (2012) 890.

[3] J.H. Snoeijer, B. Andreotti, Moving contact lines: scales, regimes, and dynamical transitions, Annu. Rev. Fluid Mech. 45 (2013) 269–292.
[4] Y. Sui, H. Ding, P.D. Spelt, Numerical simulations of flows with moving contact lines, Annu. Rev. Fluid Mech. 46 (2014) 97–119.
[5] C. Huh, L.E. Scriven, Hydrodynamic model of steady movement of a solid/liquid/fluid contact line, J. Colloid Interface Sci. 35 (1) (1971) 85–101.
[6] P.G. De Gennes, Wetting: statics and dynamics, Rev. Mod. Phys. 57 (3) (1985) 827.
[7] Y.D. Shikhmurzaev, The moving contact line on a smooth solid surface, Int. J. Multiph. Flow 19 (4) (1993) 589–610.
[8] T. Blake, J. Haynes, Kinetics of liquid/liquid displacement, J. Colloid Interface Sci. 30 (3) (1969) 421–423.
[9] T.D. Blake, The physics of moving wetting lines, J. Colloid Interface Sci. 299 (1) (2006) 1–13.
[10] M. Renardy, Y. Renardy, J. Li, Numerical simulation of moving contact line problems using a volume-of-fluid method, J. Comput. Phys. 171 (1) (2001) 243–263.
[11] Š. Šikalo, H.D. Wilhelm, I. Roisman, S. Jakirlić, C. Tropea, Dynamic contact angle of spreading droplets: experiments and simulations, Phys. Fluids 17 (6) (2005) 062103.
[12] S. Afkhami, S. Zaleski, M. Bussmann, A mesh-dependent model for applying dynamic contact angles to VOF simulations, J. Comput. Phys. 228 (15) (2009) 5370–5389.
[13] I. Malgarinos, N. Nikolopoulos, M. Marengo, C. Antonini, M. Gavaises, VOF simulations of the contact angle dynamics during the drop spreading: standard models and a new wetting force model, Adv. Colloid Interface Sci. 212 (2014) 1–20.
[14] Y. Sui, P.D. Spelt, An efficient computational model for macroscale simulations of moving contact lines, J. Comput. Phys. 242 (2013) 37–52.
[15] J.E. Sprittles, Y.D. Shikhmurzaev, Finite element simulation of dynamic wetting flows as an interface formation process, J. Comput. Phys. 233 (2013) 34–65.
[16] D. Gerlach, G. Tomar, G. Biswas, F. Durst, Comparison of volume-of-fluid methods for surface tension-dominant two-phase flows, Int. J. Heat Mass Transf. 49 (3) (2006) 740–754.
[17] K. Ritos, N. Dongari, M.K. Borg, Y. Zhang, J.M. Reese, Dynamics of nanoscale droplets on moving surfaces, Langmuir 29 (23) (2013) 6936–6943.
[18] K.G. Winkels, J.H. Weijs, A. Eddi, J.H. Snoeijer, Initial spreading of low-viscosity drops on partially wetting surfaces, Phys. Rev. E 85 (5) (2012) 055301.
[19] H. Wu, K. Fichthorn, A. Borhan, An atomistic–continuum hybrid scheme for numerical simulation of droplet spreading on a solid surface, Heat Mass Transf. 50 (3) (2014) 351–361.
[20] S.T. O'Connell, P.A. Thompson, Molecular dynamics–continuum hybrid computations: a tool for studying complex fluid flows, Phys. Rev. E 52 (6) (1995), R5792.
[21] H.S. Wijesinghe, N.G. Hadjiconstantinou, Discussion of hybrid atomistic-continuum methods for multiscale hydrodynamics, Int. J. Multiscale Comput. Eng. 2 (2) (2004) 189–202.
[22] M.K. Borg, D.A. Lockerby, J.M. Reese, A hybrid molecular-continuum simulation method for incompressible flows in micro/nanofluidic networks, Microfluid. Nanofluid. 15 (4) (2013) 541–557.
[23] W. Ren, W. E, Heterogeneous multiscale method for the modeling of complex fluids and micro-fluidics, J. Comput. Phys. 204 (1) (2005) 1–26.
[24] I.G. Kevrekidis, C.W. Gear, J.M. Hyman, P.G. Kevrekidis, O. Runborg, C. Theodoropoulos, Equation-free, coarse-grained multiscale computation: enabling microscopic simulators to perform system-level analysis, Commun. Math. Sci. 1 (4) (2003) 715–762.
[25] D.M. Holland, D.A. Lockerby, M.K. Borg, W.D. Nicholls, J.M. Reese, Molecular dynamics pre-simulations for nanoscale computational fluid dynamics, Microfluid. Nanofluid. 18 (3) (2015) 461–474.
[26] M.K. Borg, D.A. Lockerby, J.M. Reese, Fluid simulations with atomistic resolution: a hybrid multiscale method with field-wise coupling, J. Comput. Phys. 255 (2013) 149–165.
[27] T. Qian, X.P. Wang, P. Sheng, Molecular scale contact line hydrodynamics of immiscible flows, Phys. Rev. E 68 (1) (2003) 016306.
[28] W. Ren, W. E, Boundary conditions for the moving contact line problem, Phys. Fluids 19 (2) (2007) 022101.
[29] B. Qian, J. Park, K.S. Breuer, Large apparent slip at a moving contact line, Phys. Fluids 27 (9) (2015) 091703.
[30] M.K. Borg, G.B. Macpherson, J.M. Reese, Controllers for imposing continuum-to-molecular boundary conditions in arbitrary fluid flow geometries, Mol. Simul. 36 (10) (2010) 745–757.
[31] W. Nicholls, M.K. Borg, D.A. Lockerby, J.M. Reese, Water transport through carbon nanotubes with defects, Mol. Simul. 38 (10) (2012) 781–785.
[32] J. Zhang, M.K. Borg, K. Sefiane, J.M. Reese, Wetting and evaporation of salt-water nanodroplets: a molecular dynamics investigation, Phys. Rev. E 92 (5) (2015) 052403.
[33] J. Zhang, M.K. Borg, K. Ritos, J.M. Reese, Electrowetting controls the deposit patterns of evaporated salt water nanodroplets, Langmuir 32 (6) (2016) 1542–1549.
[34] M.K. Borg, D.A. Lockerby, J.M. Reese, A multiscale method for micro/nano flows of high aspect ratio, J. Comput. Phys. 233 (2013) 400–413.
[35] K. Ritos, M.K. Borg, D.A. Lockerby, D.R. Emerson, J.M. Reese, Hybrid molecular-continuum simulations of water flow through carbon nanotube membranes of realistic thickness, Microfluid. Nanofluid. 19 (5) (2015) 997–1010.
[36] M.K. Borg, D.A. Lockerby, J.M. Reese, A hybrid molecular–continuum method for unsteady compressible multiscale flows, J. Fluid Mech. 768 (2015) 388–414.
[37] O. Ubbink, Numerical Prediction of Two Fluid Systems with Sharp Interfaces (Ph.D. thesis), Imperial College London, 1997.
[38] E. Berberović, N.P. van Hinsberg, S. Jakirlić, I.V. Roisman, C. Tropea, Drop impact onto a liquid layer of finite thickness: dynamics of the cavity evolution, Phys. Rev. E 79 (3) (2009) 036306.
[39] A.A. Saha, S.K. Mitra, Effect of dynamic contact angle in a volume of fluid (VOF) model for a microfluidic capillary flow, J. Colloid Interface Sci. 339 (2) (2009) 461–480.
[40] S.S. Deshpande, L. Anumolu, M.F. Trujillo, Evaluating the performance of the two-phase flow solver interfoam, Comput. Sci. Discov. 5 (1) (2012) 014016.
[41] T. Werder, J. Walther, R. Jaffe, T. Halicioglu, P. Koumoutsakos, On the water-carbon interaction for use in molecular dynamics simulations of graphite and carbon nanotubes, J. Phys. Chem. B 107 (6) (2003) 1345–1352.
[42] D. Sergi, G. Scocchi, A. Ortona, Molecular dynamics simulations of the contact angle between water droplets and graphite surfaces, Fluid Phase Equilib. 332 (2012) 173–177.
[43] J.L. Abascal, C. Vega, A general purpose model for the condensed phases of water: TIP4P/2005, J. Chem. Phys. 123 (23) (2005) 234505.
[44] J. Brackbill, D.B. Kothe, C. Zemach, A continuum method for modeling surface tension, J. Comput. Phys. 100 (2) (1992) 335–354.
[45] D. Duvivier, D. Seveno, R. Rioboo, T. Blake, J. De Coninck, Experimental evidence of the role of viscosity in the molecular kinetic theory of dynamic wetting, Langmuir 27 (21) (2011) 13015–13021.
[46] E. Lauga, M. Brenner, H. Stone, Microfluidics: the no-slip boundary condition, in: Springer Handbook of Experimental Fluid Mechanics, Springer, 2007, pp. 1219–1240.
[47] P.A. Thompson, S.M. Troian, A general boundary condition for liquid flow at solid surfaces, Nature 389 (6649) (1997) 360–362.
[48] E. Bertrand, T.D. Blake, J. De Coninck, Influence of solid–liquid interactions on dynamic wetting: a molecular dynamics study, J. Phys.: Condens. Matter 21 (46) (2009) 464124.
[49] S. Tazi, A. Boţan, M. Salanne, V. Marry, P. Turq, B. Rotenberg, Diffusion coefficient and shear viscosity of rigid water models, J. Phys.: Condens. Matter 24 (28) (2012) 284117.
[50] Y. Nakamura, A. Carlson, G. Amberg, J. Shiomi, Dynamic wetting at the nanoscale, Phys. Rev. E 88 (3) (2013) 033010.
[51] P. Johansson, A. Carlson, B. Hess, Water–substrate physico-chemistry in wetting dynamics, J. Fluid Mech. 781 (2015) 695–711.